J|A|C|S
ARTICLES
Published on Web 12/23/2005

Photoregulated Transmembrane Charge Separation by Linked Spiropyran−Anthraquinone Molecules

Linyong Zhu,[†] Rafail F. Khairutdinov,[†] Jonathan L. Cape,[‡] and James K. Hurst*,[†]

Contribution from the Department of Chemistry and Institute of Biological Chemistry, Washington State University, Pullman, Washington 99164-4630

Received July 9, 2005; E-mail: hurst@wsu.edu

Abstract: Amide-linked spiropyran−anthraquinone (SP−AQ) conjugates were shown to mediate $ZnTPPS^{4-}$-photosensitized transmembrane reduction of occluded $Co(bpy)_3^{3+}$ within unilamellar phosphatidylcholine vesicles by external EDTA. Overall quantum yields for these reactions were dependent upon the isomeric state of the dye; specifically, 30−35% photoconversion of the closed-ring spiropyran (SP) moiety to the open-ring merocyanine (MC) form caused the quantum yield to decrease by 6-fold in the simple conjugate and 3-fold for an analogue containing a lipophilic 4-dodecylphenoxy substituent on the anthraquinone moiety. Transient spectroscopic and fluorescence quenching measurements revealed that two factors contributed to these photoisomerization-induced changes in quantum yields: increased efficiencies of fluorescence quenching of $^1ZnTPPS^{4-}$ by the merocyanine group and lowered transmembrane diffusion rates of the merocyanine-containing redox carriers. Transient spectrophotometry also revealed the sequential formation and decay of two reaction intermediates, identified as $^3ZnTPPS^{4-}$ and a species with the optical properties of a semiquinone radical. Kinetic profiles for $Co(bpy)_3^{3+}$ reduction under continuous photolysis in the presence and absence of added ionophores indicated that transmembrane redox mediated by SP-AQ was electroneutral, but reaction by the other quinone-containing mediators was electrogenic. The minimal reaction mechanism suggested from the combined studies is oxidative quenching of vesicle-bound $^3ZnTPPS^{4-}$ by the anthraquinone unit, followed by either H^+/e^- cotransport by transmembrane diffusion of SP-AQH$^\bullet$ or, for the other redox mediators, semiquinone anion-quinone electron exchange leading to net transmembrane electron transfer, with subsequent one-electron reduction of the internal $Co(bpy)_3^{3+}$. Thermal one-electron reduction of $Co(bpy)_3^{3+}$ by EDTA is energetically unfavorable; the photosensitized reaction therefore occurs with partial conversion of photonic energy to chemical and transmembrane electrochemical potentials.

Introduction

Early work from several laboratories has established that lipophilic quinones could mediate redox reactions between compartmented reactants that are phase-separated by bilayer membranes or bulk liquid membranes.[1−5] Interest in these reactions has been rekindled by recent studies from the Gust, Moore, and Moore group, who have demonstrated that assemblies containing a vectorially organized donor−sensitizer−acceptor electron transport chain and quinone pool are capable of generating a proton electrochemical gradient of sufficient magnitude to drive ATP synthesis by a membrane-incorporated F_oF_1-ATP synthase.[6,7] This latter demonstration suggests the possibility of developing energy-transducing membrane-organized systems for directed chemical syntheses that utilize solar energy. Although this area of research is often called "biomimetic" or "bioinspired", it is important to recognize that the electrogenic transmembrane redox mechanisms functioning in these systems are totally unlike the more elaborately constructed biological Q-cycles that involve transmembrane translocation of protons by membrane-localized quinones. The biological systems contain quinone-binding sites at alternate ends of membrane-spanning electron transport chains at which the quinones undergo two sequential one-electron reductions to the corresponding hydroquinones, or vice-versa.[8,9] One consequence of this organization is that protons are vectorially transported via the $Q-QH_2$ couple, thereby avoiding accumulation of O_2-reactive semiquinones. In contrast, the artificial systems lack this capability and must generate free semiquinone in photoinitiated one-electron reactions.

Mechanisms by which the quinone pool mediates transmembrane redox in these artificial systems are not well-characterized. To gain insight into these processes, we have coupled a photoisomerizable spiropyran molecule to anthraquinone, the

[†] Department of Chemistry.
[‡] Institute of Biological Chemistry.

(1) Anderson, S. S.; Lyle, I. G.; Paterson, R. *Nature* **1976**, *259*, 147−148.
(2) Grimaldi, J. J.; Boileau, S.; Lehn, J.-M. *Nature* **1977**, *265*, 229−230.
(3) Futami, A.; Hurt, E.; Hauska, G. *Biochim. Biophys. Acta* **1979**, *547*, 583−596.
(4) Joshi, N. B.; Lopez, J. R.; Tien, H. T.; Wang, C. B.; Lin, Y. Q. *J. Photochem.* **1982**, *20*, 139−151.
(5) Yablonskaya, E. E.; Klabunovskii, E. I.; Shafirovich, V. Y.; Shilov, A. E. *Dokl. Akad. Nauk SSSR* **1986**, *286*, 150−152.
(6) Steinberg-Yfrach, G.; Liddell, P. A.; Hung, S. C.; Moore, A. L.; Gust, D.; Moore, T. A. *Nature* **1997**, *385*, 239−241.
(7) Steinberg-Yfrach, G.; Rigaud, J.-L.; Durantini, E. N.; Moore, A. L.; Gust, D. A.; Moore, T. A. *Nature* **1998**, *392*, 479−482.
(8) Okamura, M. Y.; Paddock, M. L.; Graige, M. S.; Feher, G. *Biochim. Biophys. Acta* **2000**, *1458*, 148−163.
(9) Darrouzet, E.; Moser, C. C.; Dutton, P. L.; Daldal, F. *Trends Biochem. Sci.* **2001**, *26*, 445−451.

Scheme 1. Spiro(SP)−Mero(MC) Interconversion in a Spiropyran

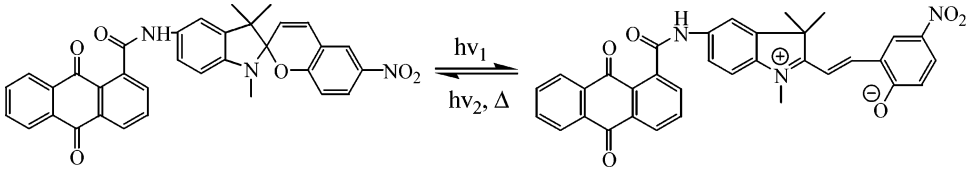

Scheme 2. Synthetic Scheme for Preparing Spiropyran−Anthraquinone Dyads

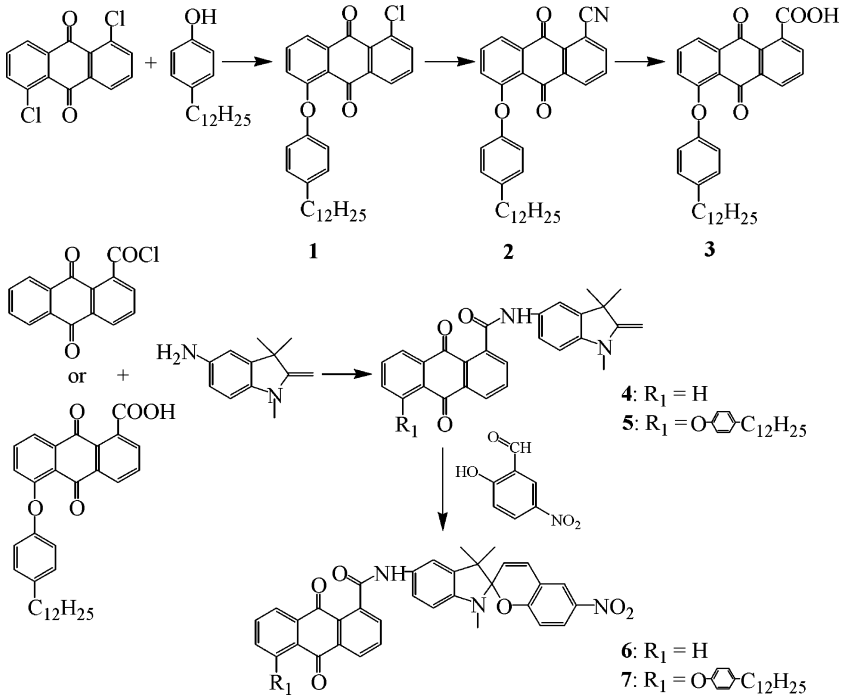

intent being to identify and achieve control of the anthraquinone location within the membrane, as well as the capability to alter its bilayer permeability. Specifically, as illustrated in Scheme 1, UV illumination induces heterolytic photocleavage of the C(spiro)−O bond, forming the more polar merocyanine form of the dye. As a consequence of its decreased lipophilicity, one expects that transmembrane diffusion of anthraquinone when appended to the mero form will be slower than when appended to the spiro form, and that the mero form will locate within a more polar microphase region of the membrane, i.e., closer to the aqueous−organic interface.[10,11] The MC forms of spiropyrans undergo thermal ring-closing at rates that can vary from several seconds to several hours, depending upon the medium and structural composition of the dye.[12,13] For the PC-solubilized MC−AQ conjugates used in this study, $t_{1/2} \approx 2$ h for ring-closing to the SP−AQ form. Ultraviolet illumination immediately prior to undertaking a kinetics experiment therefore allows one to regulate the fractional composition of the MC form in the membrane. The MC form possesses a visible absorption band, whereas the SP form does not, so that they are readily distinguishable spectroscopically. Because this band is solvatochromic,[14] the intramembrane location of MC can be estimated; because photoisomerization occurs more rapidly than molecular diffusion,[14,15] transient spectrophotometry can be used to determine the intramembrane location of SP as well, i.e., from the MC spectrum obtained immediately following flash excitation. Thus, appending spiropyrans to redox carriers allows one to manipulate the location of reactants within the microphase and the dynamics of individual reaction steps in a manner that facilitates mechanistic analysis of charge transport mechanisms.

Experimental Section

Syntheses. All chemicals were obtained from commercial suppliers as reagent grade materials and were used as received. The compound listed as 4-dodecylphenol (Aldrich) was reported upon inquiry to be a mixture of >90% 4-isomer and <8% 2-isomer. In-house deionized water was further purified using a Milli-Q ion exchange/reverse osmosis system. Linked spiropyran−anthraquinone dyads were synthesized according to the sequences summarized in Scheme 2. To prepare compound **7**, the alkylphenol was first attached to the anthraquinone via a diaryl ether bond, after which the isolated product was amide-linked to a Fischer's base containing an amino substituent. Condensation of activated anthraquinones with 5-nitrosalicylaldehyde gave the final products. Experimental details and analyses are given below.

Compound 1 (1-(4-Dodecylphenoxy)-5-chloroanthracence-9,10-dione): 2.77 g (10 mmol) of 1,5-dichloroanthraquinone and 2.8 g (11 mmol) of 4-dodecylphenol were dissolved in 30 mL of DMF, 6.9 g of K_2CO_3 were added, and the mixture was stirred overnight at 110 °C under N_2. The cooled mixture was filtered, and solvent was removed

(10) Khairutdinov, R. F.; Giertz, K.; Hurst, J. K.; Voloshina, E. N.; Voloshin, N. A.; Minkin, V. I. *J. Am. Chem. Soc.* **1998**, *120*, 12707−12713.
(11) Khairutdinov, R. F.; Hurst, J. K. *Langmuir* **2001**, *17*, 6881−6886.
(12) Bertelson, R. C. In *Organic Photochromic and Thermochromic Compounds*; Crano, J. C., Guglielmetti, R. J., Eds.; Plenum Press: New York, 1999; Vol. 1, pp 11−83.
(13) Görner, H. *Phys. Chem. Chem. Phys.* **2001**, *3*, 416−423.
(14) Minkin, V. I. *Chem. Rev.* **2004**, *104*, 2751−2776.
(15) Wilkinson, F.; Worrall, D. R.; Hobley, J.; Jansen, L.; Williams, S. L.; Langley, A. J.; Matousek, P. *J. Chem. Soc., Faraday Trans.* **1996**, *92*, 1331−1336.

from the filtrate by vacuum rotary evaporation. The residue was dissolved in CH_2Cl_2 and purified by flash column chromatography on silica gel to give 3.2 g (64%) of compound **1** as a yellow viscous fluid. ^{1}H NMR (300 MHz, $CDCl_3$): δ 0.4−1.3 (m, 25H, $C_{12}H_{25}$), 6.6 (m, 2H, 2‴,6‴-C_6H_6), 6.76 (m, 1H, 6-AQ), 6.92 (m, 2H, 3‴,5‴-C_6H_6), 7.2 (m, 2H, 3,7-AQ), 7.3 (m, 1H, 8-AQ), 7.56 (d, 1H, 2-AQ), 7.79 (m, 1H, 4-AQ) (labeling as defined for compound **7**).

Compound 2 (5-(4-Dodecylphenoxy)-9,10-dihydro-9,10-dioxoanthracence-1-carbonitrile): 3.2 g of compound **1** (6.4 mmol) and 0.85 g of cuprous cyanide (9.5 mmol) were stirred at reflux in 50 mL of dimethylacetamide for 4 h under N_2. The hot solution was poured into 700 mL of vigorously stirred water to give the copper(I) complex of the product. The crude complex was decomposed with 200 mL of boiling 4 N nitric acid for 4 h to yield 2.9 g (92%) of compound **2** as a yellow solid. ^{1}H NMR (300 MHz, $CDCl_3$): δ 0.4−1.3 (m, 25H, $C_{12}H_{25}$), 6.65 (m, 2H, 2‴,6‴-C_6H_6), 6.82−7.2 (m, 3H, 6-AQ + 3‴,5‴-C_6H_6), 7.3 (m, 2H, 3,7-AQ), 7.6 (t, 1H, 8-AQ), 7.78 (d, 1H, 4-AQ), 8.2 (d, 1H, 2-AQ) (labeling as defined for compound **7**).

Compound 3 (5-(4-Dodecylphenoxy)-9,10-dihydro-9,10-dioxoanthracence-1-carboxylic Acid): 2.8 g of compound **2** (5.7 mmol) were added to 200 mL of 70% sulfuric acid, and the mixture was stirred at reflux for 1.5 h, after which the hot solution was poured onto ice. The precipitate was collected by filtration, washed with water, and resuspended in 200 mL of CH_2Cl_2. This slurry was filtered, and the filtrate was dried over anhydrous sodium sulfate. The crude product was isolated by rotoevaporation, dissolved in 100:5 (v/v) CH_2Cl_2/CH_3-OH, and purified by flash chromatography on silica gel to give 1.3 g (45%) of compound **3**. ^{1}H NMR (300 MHz, $CDCl_3$): δ 0.4−1.3 (m, 25H, $C_{12}H_{25}$), 6.65 (m, 2H, 2‴,6‴-C_6H_6), 6.83 (s, 1H, 6-AQ), 6.92 (m, 2H, 3‴,5‴-C_6H_6), 7.15−7.4 (m, 3H, 3,7,8-AQ), 7.65 (s, 1H, 4-AQ), 7.95 (s, 1H, 2-AQ) (labeling as defined for compound **7**).

Compound 4 (9,10-Dihydro-*N*-(1,3,3-trimethyl-2-methyleneindolin-5-yl)-9,10-dioxoanthracene-1-carboxamide): A mixture of 1.73 g (9.2 mmol) of 5-amino-1,3,3-trimethyl-2-methyleneindoline, 1.98 g (9.2 mmol) of Proton-Sponge (1,8-bis(dimethylamino)naphthalene), and 2.5 g (9.2 mmol) of anthraquinone-1-carbonyl chloride in 150 mL of dry THF was stirred overnight at room temperature under N_2. Following filtration, the crude product was isolated from the filtrate by rotoevaporation and purified after dissolution in 100:3 (v/v) CH_2Cl_2/CH_3OH and flash column chromatography on silica gel to give 1.9 g (52%) of compound **4**. ^{1}H NMR (300 MHz, $CDCl_3$): δ 1.32 (s, 6H, 8″,8″-CH_3-indoline), 3.03 (s, 3H, 1″-CH_3-indoline), 3.85 (s, 2H, 9″-CH_2-indoline), 6.43 (d, 1H, 3″-indoline), 7.36 (dd, 1H, 4″-indoline), 7.51 (d, 1H, 6″-indoline), 7.76 (m, 2H, 6,7-AQ), 8.2 (m, 2H, 5,8-AQ), 8.28 (m, 2H, 3,4-AQ), 8.42 (s, 1H, NH), 8.59 (d, 1H, 2-AQ) (labeling as defined for compound **6**).

Compound 5 (5-(4-Dodecylphenoxy)-9,10-dihydro-*N*-(1,3,3-trimethyl-2-methyleneindolin-5-yl)-9,10-dioxoanthracene-1-carboxamide): A solution of 6 g (11.7 mmol) of compound **3** and 2.22 g (12.6 mmol) of 2-chloro-4,6-dimethoxy-1,3,5-triazine in 150 mL of dry THF was stirred in an ice bath under N_2. 1.35 mL (12.6 mmol) of *N*-methylmorpholine was then slowly syringe-injected at 4 °C. The filtrate from this reaction was then added to 1.47 g (7.8 mmol) of 5-amino-1,3,3-trimethyl-2-methyleneindoline and 1.35 mL (12.6 mmol) of *N*-methylmorpholine in 50 mL of THF. This solution was stirred at 4 °C for 2 h and then warmed to room temperature for 24 h. After removal of solvent, the residue was dissolved in 100:3 (v/v) CH_2Cl_2/CH_3OH and purified by flash column chromatography on silica gel to give 2.8 g (52.5%) of compound **5**. ^{1}H NMR (300 MHz, $CDCl_3$): δ 0.3−1.4 (m, 31H, $C_{12}H_{25}$ + 8″,8″-CH_3-indoline), 3.03 (s, 3H, 1″-CH_3-indoline), 3.85 (s, 2H, 9″-CH_2-indoline), 6.42 (d, 1H, 3″-indoline), 6.96 (m, 2H, 2‴,6‴-C_6H_6), 7.07 (s, 1H, 6-AQ), 7.2−7.4 (m, 4H, 3‴,5‴-C_6H_6 + 4″,6″-indoline), 7.4−7.68 (m, 3H, 3,7,8-AQ), 7.9 (m, 1H, 4-AQ), 7.98 (s, 1H, 2-AQ), 8.04 (s, 1H, NH) (labeling as defined for compound **7**).

Compound 6 (9,10-Dihydro-*N*-(1,3-dihydro-1,3,3-trimethyl-6-nitrospiro[2*H*-1-benzopyran-2,2′-(2*H*)-indole])-9,10-dioxoanthracene-1-carboxamide) (SP−AQ): A solution of 1.08 g (2.6 mmol) of compound **4** and 0.43 g (2.6 mmol) of 2-hydroxy-5-nitrobenzaldehyde in 200 mL of MeOH was refluxed for 4 h. After removal of solvent by rotoevaporation, the residue was dissolved in 100:3 (v/v) CH_2Cl_2/CH_3-OH and purified by flash chromatography on silica gel to give 1.02 g (67%) of compound **6** (SP−AQ) (mp > 200 °C). MS *m*/*z* 571.5. Calcd

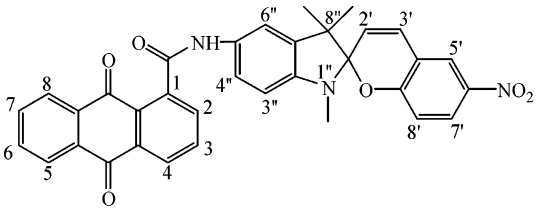

for $C_{34}H_{25}N_3O_6$: C, 71.44; H, 4.41; N, 7.35. Found: C, 71.28; H, 4.84; N, 7.14. ^{1}H NMR (300 MHz, d^6-DMSO): δ 1.15 (s, 3H, 8″-CH_3-indoline), 1.23 (s, 3H, 8″-CH_3-indoline), 2.67 (s, 3H, 1″-CH_3-indoline), 6.01 (d, 1H, 2′-oxazine), 6.64 (d, 1H, 3″-indoline), 6.9 (d, 1H, 3′-oxazine), 7.35 (d, 1H, 8′-oxazine), 7.58 (m, 2H, 4″,6″-indoline), 7.9−8.05 (m, 3H, 3,6,7-AQ), 8.2−8.5 (m, 5H, 2,4,5,8-AQ; 7′-oxazine), 8.78 (s, 1H, 5′-oxazine), 10.55(s, 1H, NH).

Compound 7 (5-(4-Dodecylphenoxy)-9,10-dihydro-*N*-(1,3-dihydro-1,3,3-trimethyl-6-nitrospiro[2*H*-1-benzopyran-2,2′-(2*H*)-indole])-9,10-dioxoanthracene-1-carboxamide) (SP−AQ−C_{12}): A solution of 0.205 g (0.3 mmol) of compound **5** and 0.05 g (0.3 mmol) of 2-hydroxy-5-nitrobenzaldehyde in 20 mL of MeOH was refluxed for 4 h. After removal of solvent by rotoevaporation, the residue was dissolved in 100:2 (v/v) CH_2Cl_2/CH_3OH and purified by flash chromatography on silica gel to give 0.1 g (40%) of compound **7** (SP−AQ−C_{12}) (mp 112−114.5 °C). MS *m*/*z* 831.9. Calcd for $C_{52}H_{53}N_3O_7$: C, 75.07; H, 6.42;

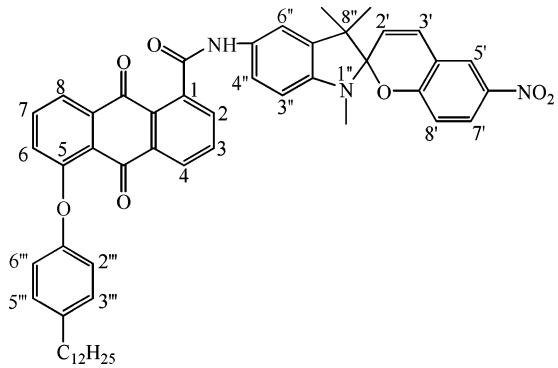

N, 5.05. Found: C, 74.89; H, 6.40; N, 5.20. ^{1}H NMR (300 MHz, $CDCl_3$): δ 0.3−1.5 (m, 31H, $C_{12}H_{25}$ + 8″,8″-CH_3-indoline), 2.72 (s, 3H, 1″-CH_3-indoline), 5.85 (d, 1H, 2′-oxazine), 6.48 (d, 1H, 3″-indoline), 6.8 (dd, 2H, 2‴,6‴- C_6H_6), 7.02 (d, 2H, 3‴,5‴-C_6H_6), 7.11 (m, 1H, 3′-oxazine), 7.3 (m, 2H, 8′-oxazine + 4″-indoline), 7.4−7.68 (m, 5H, 6″-indoline + 3,6,7,8-AQ), 7.9−8.12 (m, 4H, 2,4,-AQ + NH + 7′-oxazine), 8.42 (s, 1H, 5′-oxazine).

^{13}C NMR spectra for all of the synthesized compounds are given in the Supporting Information. 9,10-Anthraquinone was reduced to the corresponding diol by H_2O_2-induced reduction with sodium borohydride, as described in the literature.[16]

Vesicle Preparation. Phosphatidylcholine (PC) was extracted from fresh hen's egg yolk and purified by column chromatography following literature procedures.[17] Aqueous suspensions of PC and the dopants (SP, AQ, SP−AQ, or SP−AQ−C_{12}) in 40 mM Tris buffer, pH 8.0,

(16) Panson, G. S.; Weill, C. E. *J. Am. Chem. Soc.* **1955**, *22*, 120−121.
(17) Singleton, W. S.; Gray, M. S.; Brown, M. L.; White, J. L. *J. Am. Oil Chem. Soc.* **1965**, *42*, 53−56.

were formed by first mixing the components in $CHCl_3$ and rotoevaporating the solution to form a surfactant surface film, which was then detached from the flask and hydrated by introduction of the aqueous buffer and repeated freeze−thaw cycling. Unilamellar vesicles with average diameters of 100 nm were prepared by high-pressure extrusion;[18] dopant molecule/PC vesicle ratios used in the various experiments ranged from ∼25−3000.

Optical Measurements. Continuous photolysis experiments were performed using filtered light from a 1.5-kW xenon lamp. For experiments involving spiro ⇌ mero photoisomerization, aqueous $CuSO_4$ and either Schott UG11 or Corning OG590 filters were used to provide broadband illumination in the UV (260 nm < λ < 390 nm) or visible (540 nm < λ < 650 nm) regions, respectively. For quantum yield measurements a narrow band-pass interference filter with transmission at 420 nm was used to selectively excite the Soret band of $ZnTPPS^{4-}$. The filtered light was then passed via an optical fiber bundle to a reaction cuvette that was mounted in a Hewlett-Packard 8452 diode array spectrophotometer interfaced to a ChemStation data acquisition/analysis system. Light intensities were measured with a calibrated PowerMax 500D laser power meter maintained at room temperature; with the UG11 filter in place, the values obtained were $(0.5-5) \times 10^{-8}$ einstein/(cm^2 s).

Absorption spectra and decay kinetics of photoinduced intermediates were measured by laser flash photolysis using a transient spectrophotometer whose general characteristics have been described.[19] The third harmonic (355 nm) from a Continuum Surelite III Nd:YAG laser was used as the excitation source; optical absorbances of samples at 355 nm were maintained below 0.1. Fluorescence measurements were made using a SPEX Fluorolog-3 spectrofluorometer.

Other Measurements. Mass spectra were determined by MALDI-TOF in 2,5-dihydroxybenzoic acid using an Applied Biosystems Voyager DE RP instrument.

Cyclic voltammograms were obtained in dry dimethyl sulfoxide solutions containing 0.1 M tetrabutylammonium tetrafluoroborate using a Princeton Applied Research model 273 potentiostat/galvanostat. Measurements were made in a standard two-compartment, three-electrode cell consisting of a glassy carbon working electrode, a coiled platinum wire auxiliary electrode, and a Ag/0.1 M $AgNO_3$ reference electrode in DMSO, which was isolated from the reaction chamber by a Vycor frit. Half-cell potentials were measured at scan rates of 50−200 mV s^{-1}; ferrocene was added as an internal redox standard.

The extent of binding of $ZnTPPS^{4-}$ to the PC vesicles was determined by ultrafiltration using Centricon-10 centrifugal microconcentrators.[19] This method relies upon forcing solution through a semipermeable membrane (in this case, one with a 10 000 molecular-weight cutoff), which permits unrestricted passage of unbound $ZnTPPS^{4-}$ but prevents permeation by the vesicles and any $ZnTPPS^{4-}$ bound to them. Comparison of $ZnTPP^{4-}$ concentrations in the exudate and retentate allows direct measurement of the fraction that is bound. In a typical experiment, 2.5 mL of a vesicle suspension containing $ZnTPPS^{4-}$ was spun for 2.5 min at 4000 rpm in a Sorvall RC-2B refrigerated centrifuge fitted with an SS-34 rotor (∼5800 g). Under these conditions, about 0.1 mL of solution containing unbound $ZnTPPS^{4-}$ passed through the membrane and was collected. Because less than 5% of the solution volume was allowed to pass through the membrane during sample collection, the vesicle concentration in the retentate was essentially unchanged; consequently, the concentration of $ZnTPPS^{4-}$ in the exudate could be taken as equal to that of the unbound reagent in the retentate. The portion of PC-bound $ZnTPPS^{4-}$ in retentate was then calculated as the difference in total concentrations of $ZnTPPS^{4-}$ in the filtrate and retentate, measured spectrophotometrically at the Soret band maximum ($\epsilon_{421} = 6.8 \times 10^5$ M^{-1} cm^{-1}).[20]

Computational Methods. All calculations were performed in the Gaussian 03 suite of programs.[20] Ab initio determination of the redox potential for the anthraquinone moiety of compound **7** was determined using the method of Fu and co-workers.[21] Geometry optimizations and frequency calculations of compound **7** truncated with methyl ether and dimethyl amino groups at positions 5 and 5″, respectively, were carried out at the B3LYP/6-31G(d, p) level. Single-point energy calculations using the PCM solvation model were carried out at the B3LYP/6-311G-(d, p) level using dielectric constants of 78 (water), 46 (dimethyl sulfoxide), 36.4 (acetonitrile), 20.7 (acetone), 8.9 (methylene chloride), 4.9 (chloroform), and 2 (cyclohexane). All redox potentials are referenced the Fc^+/Fc couple extrapolated to the dielectric of DMSO ($E° = 0.570$ V vs NHE).[22]

Results and Discussion

Photochromic Behavior of SP−AQ Dyads in PC Vesicles. In earlier studies, we had found that simple amphiphilic spiropyrans and structurally similar spirooxazines underwent reversible photoinitiated ring-opening−closing reactions, as well as thermal ring-closing reactions, that were similar to those occurring in homogeneous solution.[10,11] However, one distinguishing feature of the reactions in vesicles is that rapid ring-opening[14,15] was often followed by a slower reaction on millisecond time scales. This reaction was not observed for the corresponding reactions when vesicles were absent and was attributed to intramembrane structural reorganization following generation of the more polar MC form of the dye. From the solvatochromic properties of the MC visible band, we inferred that this step involved an increase in the medium polarity surrounding the dye; this could arise from either physical disruption of the membrane bilayer structure, allowing greater access by solvent, or relocation of the dye itself from the nonpolar membrane interior toward the membrane-aqueous interface. Rates of K^+ efflux from SP-containing DHP vesicles were found to decrease upon photoisomerization to the MC form, consistent with the latter, but not the former, interpretation.[11]

SP−AQ and SP−AQ−C_{12} are water insoluble and are strongly incorporated into PC vesicles during their formation. The photoresponses of both these compounds in the vesicles to continuous illumination were comparable to those observed for simple PC-bound spiropyrans.[11] The nature of the optical changes that occurred is illustrated for SP−AQ in Figure 1, where the spectra obtained under ultraviolet and visible illumination are compared. These transformations were fully reversible over several alternating cycles of UV and visible light, and conversion rates were proportional to the intensities of illuminating light. Slow thermal ring-closing also occurred, which in PC liposomes followed first-order decay with an apparent rate constant of $k = 9 \times 10^{-5}$ s^{-1} at 23 °C. The MC visible absorption maxima were used to estimate the microphase location of the chromophores within the membrane. The positions of these bands in homogeneous solutions exhibited an approximately linear dependence upon the solvent dielectric constant (ϵ) over the range $\epsilon = 2-32$, i.e., $\lambda_{max} = a_1 + a_2 \times$

(18) Mayer, L. D.; Hope, M. J.; Cullis, P. R. *Biochim. Biophys. Acta* **1986**, *858*, 161−168.
(19) Lymar, S. V.; Khairutdinov, R. F.; Soldatenkova, V. A.; Hurst, J. K. *J. Phys. Chem. B* **1998**, *102*, 2811−2819.
(20) Kalyanasundaram, K.; Neumann-Spallart, M. *J. Phys. Chem.* **1982**, *86*, 5163−5169.
(21) R. C., Frisch, M. J.; et al. *Gaussian 03*; Gaussian, Inc.: Wallingford CT, 2004 (complete citation given in the Supporting Information).
(22) Fu, Y.; Liu, L.; Yu, H. Z.; Wang, Y. M.; Guo, Q. X. *J. Am. Chem. Soc.* **2005**, *127*, 7227−7234.

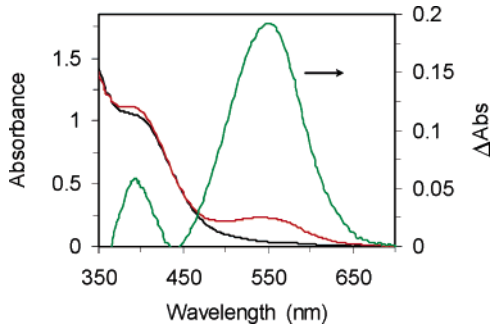

Figure 1. Absorption spectra of SP−AQ in PC vesicles under continuous illumination with filtered UV (red) and visible light (black). The merocyanine−spyropyran difference absorption spectrum is given in green. Conditions: 0.23 mM SP−AQ, ∼80 nM PC (5 mg/mL) in 40 mM Tris/Cl, pH 8.0.

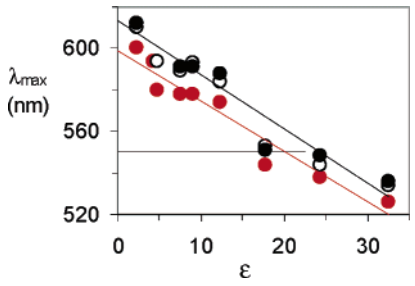

Figure 2. Dependence of λ_{max} for MC (red circles), MC−AQ (black closed circles), and MC−AQ−C_{12} (black open circles) upon the solvent dielectric constant (ϵ). The solvents used were as follows: cyclohexane (2.03), chloroform (4.8), tetrahydrofuran (7.6), dichloromethane (9.08), pyridine (12.4), 2-propanol (18.3), ethanol (24.3), and methanol (32.6).

ϵ.[10,11] This relationship is illustrated in Figure 2, for which best fit values to the experimental data were obtained with a_1 = 599 nm and a_2 = −2.5 nm for SP and a_1 = 613 nm and a_2 = −2.6 nm for SP−AQ and SP−AQ−C_{12}. The positions of the MC visible band maxima in PC vesicles are ∼500 nm for SP, ∼550 nm for SP−AQ, and ∼600 nm for SP−AQ−C_{12}. These values were used to estimate apparent dielectric constants of 40, 25, and 6, respectively, of the chromophore environments within the bilayer (e.g., the horizontal line in Figure 2 representing λ_{max} for SP−AQ intersects the upper line at ϵ = 25). Modeling studies suggest that the dielectric strength drops precipitously across the headgroup region of PC bilayers from a value of ϵ = 78 in bulk H_2O to $\epsilon \approx 6$ within the acylcarbonyl groups of the glycerol backbone, a lateral distance of ∼0.5 nm.[24−26] Within the ∼3.0 nm thick interior hydrocarbon portion of the bilayer, the dielectric strength is relatively constant with $\epsilon < 5$. The positions of the MC bands are therefore sensitive indicators of relatively small changes in microenvironments within the interfacial region of the membrane. The data suggest that attachment of the anthraquinone and dodecylphenoxy units to SP cause progressive displacement of SP−AQ and SP−AQ−C_{12} toward the membrane interior, which is consistent with the hydrophobic nature of these substituents.

Transient spectroscopy revealed that the visible bands of MC and MC−AQ−C_{12} in PC vesicles immediately following laser flash-induced SP → MC photoisomerization were red-shifted relative to their equilibrium values, although virtually no temporal change was observed in the initially formed MC−AQ (Figure 3).

The kinetic response following flash excitation is illustrated in Figure 4 for SP-containing PC vesicles. The initial rapid rise in absorbance, which occurred within the rise time of our instrument, can be attributed to initial ring-opening steps and subsequent equilibration of isomeric merocyanine forms. In homogeneous solution, these reactions are complete within the first millisecond following flash excitation.[13−15] The slow step, which we attribute to environmental relaxation within the vesicle, exhibited first-order decay with relaxation times at 23 °C of τ = 0.3 ms for MC and τ = 1.2 ms for MC−AQ−C_{12}. The relatively slow relaxation time and smaller spectroscopic shift of MC−AQ−C_{12}, as well as the absence of a detectable relaxation for MC−AQ, may reflect "anchoring" effects of the lipophilic substituents, which would thermodynamically oppose movement of the molecule toward the more polar microphase regions of the bilayer.

Fluorescence Quenching of ZnTPPS^{4-}. Although ZnTPPS^{4-} is nominally water-soluble, ultrafiltration studies indicated that, under the conditions of these studies, 80 ± 5% of the zinc porphyrin was bound to the formally neutral PC vesicles. This behavior is consistent with previous measurements reported for PC vesicle suspensions[27] but differs markedly from that of similar suspensions of anionic dihexadecyl phosphate (DHP) vesicles, where electrostatic repulsion between ZnTPPS^{4-} and the negatively charged membrane interface precludes substantive adsorption of the metalloporphyrin.[28] Addition of SP caused no change in the intrinsic ZnTPPS^{4-} fluorescence from either methanolic solutions or aqueous suspensions of PC vesicles. However, as illustrated in Figure 5a, partial conversion to MC by preillumination with UV light did cause significant quenching of the porphyrin fluorescence. The energy of the first excited singlet state of PC vesicle-bound ZnTPPS^{4-} was estimated to be 2.07 eV from the average of frequencies of the Q(0,0) absorption and emission bands. Similar calculations based upon absorption and emission maxima gave first-excited singlet energies of 2.25, 2.13, and 1.98 eV for vesicle-bound MC, MC−AQ, and MC−AQ−C_{12}, respectively. Some uncertainty is introduced in the latter numbers because the distribution of isomeric merocyanine forms[14,15,29] is probably different for the absorbing and fluorescing species.

Nonetheless, these data suggest that fluorescence quenching of ^{1}ZnTPPS^{4-} by MC is not efficient, since it would be endergonic by ∼200 mV in PC vesicles. This conclusion differs from that reached in a similar study of a zinc porphyrin dyad containing a structurally analogous spiropyran unit, where quenching was attributed to porphyrin → merocyanine energy transfer.[29]

To provide an estimate of the electrochemical potentials for the various redox-active components in vesicles, half-wave potentials were measured in DMSO by cyclic voltammetry. Irreversible one-electron reduction and oxidation waves assignable to the spiropyran moiety were clearly evident in the voltammograms, consistent with earlier reports;[30] reduction

(23) Zuman, P.; Meites, L. *Electrochemical Data*; *Vol. A.*; John Wiley & Sons: New York, 1974.
(24) Mazeres, S.; Schramm, V.; Tocanne, J.; Lopez, A. *Biophys. J.* **1996**, *71*, 327−335.
(25) Wiener, M. C.; White, S. H. *Biophys. J.* **1992**, *61*, 434−447.
(26) Sanders, C. R., II.; Schwonek, J. P. *Biophys. J.* **1993**, *65*, 1207−1218.
(27) Kuhn, E. R.; Hurst, J. K. *J. Phys. Chem.* **1993**, *97*, 1712−1721.
(28) Hurst, J. K.; Lee, L. Y.-C.; Grätzel, M. *J. Am. Chem. Soc.* **1983**, *105*, 7048−7056.
(29) Bahr, J. L.; Kodis, G.; de la Garza, L.; Lin, S.; Moore, A. L.; Moore, T. A.; Gust, D. *J. Am. Chem. Soc.* **2001**, *123*, 7124−7133.

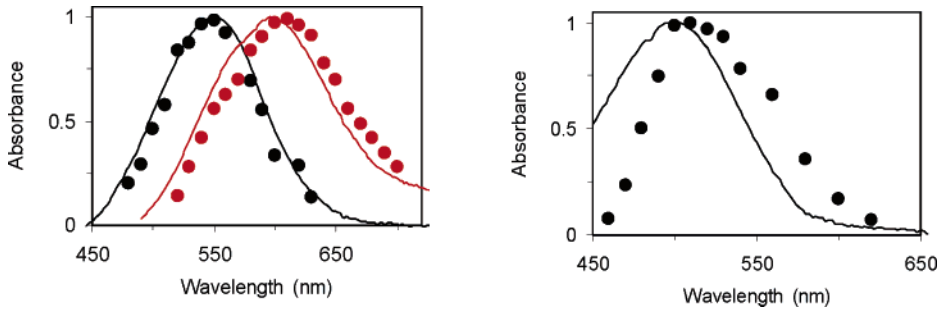

Figure 3. Normalized absorption spectra of PC vesicles containing (left panel) MC−AQ (black) or MC−AQ−C_{12} (red) or (right panel) MC. Solid circles are normalized absorbance changes measured at 10^{-6} s after applying a 5 mJ 355 nm laser pulse; solid lines are normalized absorption spectra obtained after 100 s of continuous UV illumination of the same suspensions. Conditions: [SP], [SP−AQ], or [SP−AQ−C_{12}] = 0.23 mM, [PC] ≈ 80 nM (5 mg/mL) in 40 mM Tris/Cl, pH 8.0.

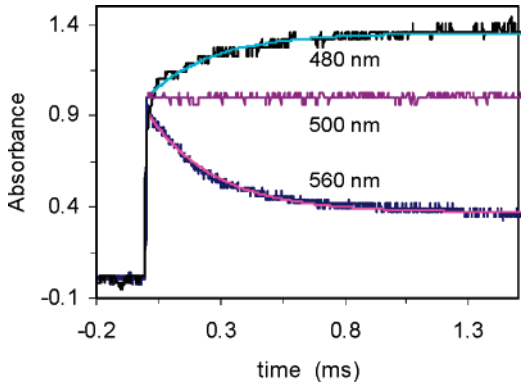

Figure 4. Normalized transient absorbance decay kinetics at 480, 500, and 580 nm of SP-doped PC vesicles. Data are averages of 8 individual experiments. The solid lines are calculated curves using $\Delta Abs = 1 + b(1 - \exp(-t/\tau))$, where b is the wavelength-dependent value of the total amplitudinal change. Conditions: 0.23 mM SP, ~80 nM PC (5 mg/mL) in 40 mM Tris/Cl, pH 8.0, 23 °C.

waves for the AQ unit were reversible, indicating a simple one-electron reaction at the electrode to the AQ semiquinone anion. Half-wave potentials, referenced against the $Fc^{+/0}$ couple, are listed in Figure 6. No difference was observed in either oxidation or reduction waves when SP solutions were ~70% photoisomerized to MC or when SP−AQ solutions were ~40% photoisomerized to MC−AQ, suggesting that the potentials for the ring-open and ring-closed forms were nearly identical; this observation is consistent with previous reports on the redox properties of similar spiropyrans.[29,31] The appended AQ unit had no effect upon the apparent $E_{1/2}$ for SP or MC reduction; however, it did cause the SP(MC) oxidation wave to shift cathodically by almost 200 mV (Figure 6). Based upon these potentials, it appears that oxidative quenching of $^1ZnTPPS^{4-}$ by MC (and SP), i.e.,

$$^1ZnTPPS^{4-} + MC\ (SP) \rightarrow ZnTPPS^{3-} + MC^{\bullet-}\ (SP^{\bullet-}) \quad (1)$$

is thermodynamically feasible ($\Delta E \approx 0.07$ V) but that reductive quenching is not ($\Delta E \approx -0.30$ V). The absence of $^1ZnTPPS^{4-}$ quenching by vesicle-bound SP, which should also be thermodynamically allowed, might be attributed to greater penetration of the bilayer by SP, which could increase the effective electron-transfer distance, thereby causing the redox reaction to become noncompetitive with normal deactivation pathways, or could shift the $SP^{0/-}$ potential to lower values as a consequence of relocation to a less polar environment within the microphase. However, these explanations cannot account for the differing quenching capabilities of MC and SP in methanol. A Stern−Volmer analysis was made of the quenching of $^1ZnTPPS^{4-}$ fluorescence intensities by MC in methanol, i.e., using the equation $I_o/I = 1 + k_q[MC]\tau$, where the fluorescence lifetime (τ) is 1.6 ns.[20] These analyses gave calculated bimolecular quenching rate constants ($k_q > 1 \times 10^{13}$ M^{-1} s^{-1}) that were several orders of magnitude above the diffusional limit of ~2×10^{10} M^{-1} s^{-1}, excluding dynamic quenching and implying a mechanism involving static quenching within associated species. Aggregation of bound reactants is a common feature of vesicle-organized systems[28,32−35] that could also complicate thermodynamic analyses of these reactions. Thus, for all these reasons, the conclusion that fluorescence quenching of $^1ZnTPPS^{4-}$ by MC and SP is primarily oxidative must be regarded as tentative.

When the spiropyran is covalently linked to an anthraquinone, both ring-open and ring-closed forms of the dye are capable of quenching $^1ZnTPPS^{4-}$; from the data presented in Figure 5b, the relative quenching efficiencies in PC vesicles are estimated as MC−AQ > MC−AQ−C_{12} ≈ SP−AQ > SP−AQ−C_{12}. The acquired capacity for quenching by the ring-closed SP compounds may reflect one-electron transfer directly from $^1ZnTPPS^{4-}$ to the appended AQ moiety. Based upon the potentials given in Figure 6, the reaction

$$^1ZnTPPS^{4-} + SP{-}AQ \rightarrow ZnTPPS^{3-} + SP{-}AQ^{\bullet-} \quad (2)$$

should be exothermic by ~0.5 V. In contrast, singlet−singlet energy transfer to either the SP or AQ units is unfavorable by at least 1 V, based upon the position of the lowest-energy absorption band in PC vesicles (~400 nm (Figure 1), for which $E \approx 3.1$ eV). In support of reaction 2, ~15% quenching of $^1ZnTPPS^{4-}$ fluorescence was also observed when an equivalent amount of AQ was incorporated into the vesicles (data not shown). Singlet−singlet energy transfer from $^1ZnTPPS^{4-}$ is considerably less endergonic for MC−AQ than MC and is exergonic for MC−AQ−C_{12}. In principle, then, all three mechanisms (energy transfer to MC and oxidative quenching

(30) Alberti, A.; Barberis, C.; Campredon, M.; Gronchi, G.; Guerra, M. *J. Phys. Chem.* **1995**, *99*, 15779−15784.
(31) Zhi, J. F.; Baba, R.; Hashimoto, K.; Fujishima, A. *J. Photochem. Photobiol. A* **1995**, *92*, 91−97.
(32) Cellarius, R. A.; Mauzerall, D. *Biochim. Biophys. Acta* **1966**, *112*, 235−255.
(33) Kunitake, T.; Ihara, H.; Okahata, Y. *J. Am. Chem. Soc.* **1983**, *105*, 6070−6078.
(34) Nakashima, N.; Morimitsu, K.; Kunitake, T. *Bull. Chem. Soc. Jpn.* **1984**, *57*, 3252−3257.
(35) Yamazaki, I.; Tamai, N.; Yamazaki, T. *J. Phys. Chem.* **1990**, *94*, 516−525.

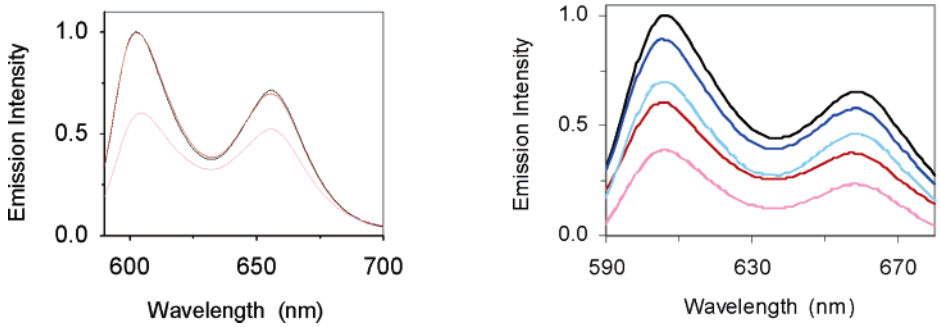

Figure 5. Normalized emission spectra of $ZnTPPS^{4-}$ in PC vesicle solutions. (a) (black) no quencher; (red) [SP] = 20 μM; (pink) [SP] = 6 μM, [MC] = 14 μM. (b) (black) no quencher; (blue) [SP−AQ−C_{12}] = 20 μM; (light blue) [SP−AQ−C_{12}] = 14 μM, [MC−AQ−C_{12}] = 6 μM; (red) [SP−AQ] = 20 μM; (pink) [SP−AQ] = 13 μM, [MC−AQ] = 7 μM. All experiments were in 40 mM Tris/Cl, pH 8.0, with [PC] ≈ 80 nM (5 mg/mL).

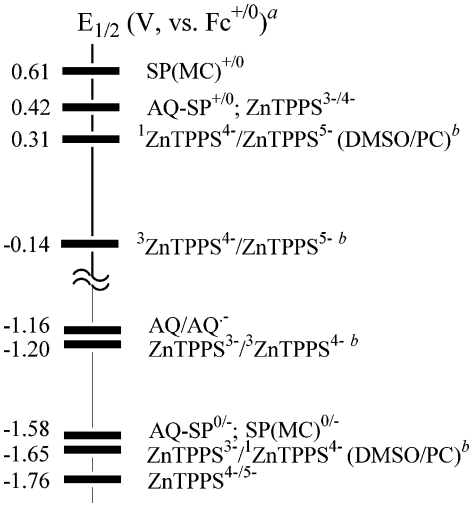

Figure 6. Half-cell potentials for redox components in DMSO. [a]$E_{1/2}(Fc^{+/0})$ = +0.13 V vs Ag/0.1M $AgNO_3$(DMSO); [b]estimated from the $ZnTPPS^{4-}$ first excited singlet (2.07 V (PC vesicles)) and triplet state (1.62 V[20]) energies.

by both MC and AQ) could contribute to fluorescence quenching in these systems.

Quenching of ^{3}ZnTPPS^{4-} by SP. The intrinsic lifetime of $^3ZnTPPS^{4-}$ was determined by transient spectroscopy to be τ = 2.1 ms in both methanol and PC vesicle suspensions; under the prevailing experimental conditions, decay of $^3ZnTPPS^{4-}$ at its absorption maximum of 460 nm was single-exponential, indicating negligible contribution from bimolecular pathways[36] or vesicle-bound aggregated porphyrins.[28]

Addition of SP to methanolic solutions caused the $^3ZnTPPS^{4-}$ decay rate to increase, although the waveform remained single-exponential; addition of SP to vesicles also increased the decay rate, with the waveform now appearing markedly biexponential (Figure 7). The energy of the first-excited triplet state of SP (~2.1 eV)[37] is considerably above that of $^3ZnTPPS^{4-}$ (~1.6 eV),[19] so that triplet−triplet energy transfer is unlikely to be the quenching mechanism. However, based upon the data in Figure 6, both oxidative quenching ($\Delta E \approx -0.38$ V) and reductive quenching ($\Delta E \approx -0.75$ V) are also energetically unfavorable. Apparently, the greater reactivity of $^3ZnTPPS^{4-}$ than $^1ZnTPPS^{4-}$ toward SP can be attributed to the 10^6-fold greater lifetime of the triplet-excited state, whose very slow normal decay pathways allow expression of relatively inefficient

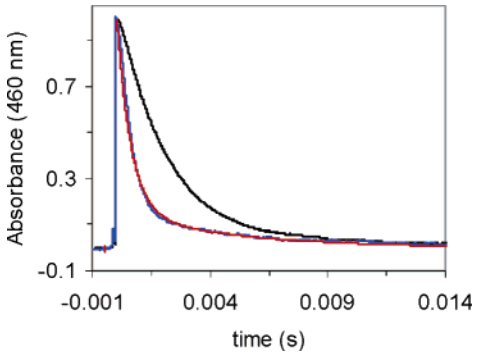

Figure 7. Normalized decay kinetics at 460 nm of the transient absorption following photoexcitation of $ZnTPPS^{4-}$ in suspensions of PC liposomes (black) and SP-containing PC liposomes (blue). The red line is a biexponential fit of the experimental data with τ_1 = 0.5 ms and τ_2 = 1.4 ms. Conditions: [PC] ≈ 80 nM (5 mg/mL), [SP] = 0.23 mM (when present), in 40 mM Tris/Cl, pH 8.0, 23 °C.

quenching processes. Indeed, the rate constant calculated for the triplet quenching reaction in methanol at 23 °C was only $k_q = 5 \times 10^7$ M^{-1} s^{-1}, which is compatible with an activation barrier of several hundred millivolts. For this reaction, then, the most likely quenching mechanism is oxidative, i.e.:

$$^3ZnTPPS^{4-} + SP \rightarrow ZnTPPS^{3-} + SP^{\bullet-} \qquad (3)$$

The $^3ZnTPPS^{4-}$ decay kinetics in SP-doped vesicle suspensions obeyed the equation: $A_{460}(t) = A_1 \exp(-t/\tau_1) + A_2 \exp(-t/\tau_2)$ (Figure 7); best-fit values of the parameters obtained were $A_1/(A_1 + A_2) = 0.85$, $\tau_1 = 0.5$ ms, and $\tau_2 = 1.4$ ms. Quenching of $^3ZnTPPS^{4-}$ by the vesicle-bound SP could, in principle, involve either or both vesicle-bound and aqueous fractions of the zinc porphyrin. Specifically, the calculated relaxation time for a diffusion-limited bimolecular reaction between $ZnTPPS^{4-}$ and the vesicles under the experimental conditions[38] is $\tau \approx 30$ μs, which is an order of magnitude larger than the intrinsic $^3ZnTPPS^{4-}$ lifetime. However, the rate constant for reaction between $^3ZnTPPS^{4-}$ and SP in methanol is 10^4-fold smaller than the calculated diffusion-limited constant for

(36) Pekkarinen, L.; Linschitz, H. *J. Am. Chem. Soc.* **1960**, *82*, 2407−2411.
(37) Lashkov, G. I.; Ermolaev, V. L.; Shanlya, A. V. *Opt. Spektrosk.* **1966**, *21*, 546−549.

(38) The diffusion-limited bimolecular quenching constant (k_d) can be estimated from the Debye equation, $k_d \approx (4 \times 10^{-3})\pi \times R_v \times D \times N_o$, where R_v is the vesicle radius, D is the $^3ZnTPPS^{4-}$ aqueous diffusion coefficient, and N_o is Avogadro's number. When $R_v = 5 \times 10^{-6}$ cm and $D = 2 \times 10^5$ cm^2/s, $k_d = 7.5 \times 10^{11}$ M^{-1} s^{-1}. The corresponding relaxation time, defined as $\tau_d = (k_d \times [PC])^{-1}$, is 33 μs when the effective concentration of vesicles ([PC]) is 8×10^{-8} M. Assuming that the average molecular weight of the PC surfactant monomers is 730 amu and that their cross-sectional areas in the outer and inner bilayer leaflets are 0.74 nm^2 and 0.61 nm^2, respectively [Huang, C.; Mason, J. T. *Proc. Natl. Acad. Sci. U.S.A.* **1978**, *75*, 308−310], this concentration corresponds to 5 mg/mL PC.

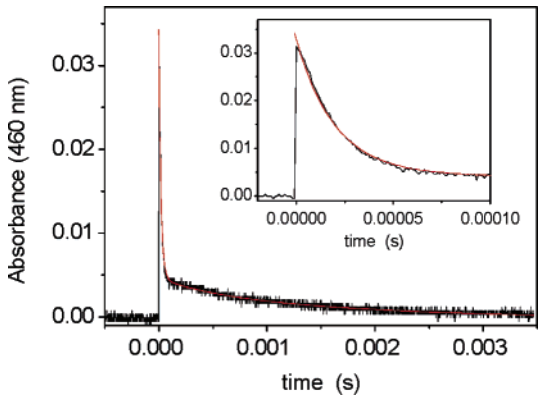

Figure 8. Decay of transient absorption at 460 nm following photoexcitation of $ZnTPPS^{4-}$ in a (SP−AQ)-containing PC vesicle solution. The initial phase of the decay curve is shown in the insert. The red line is a biexponential fit with $\tau_1 = 20$ μs and $\tau_2 = 1.7$ ms. Conditions are the same as those given in Figure 7.

the reaction with vesicles ($k_d = 8 \times 10^{11}$ M^{-1} s^{-1}).[38] One might therefore reasonably assume that electron transfer from the vesicle-bound SP is also relatively slow and consequently that $^3ZnTPPS^{4-}$ quenching only occurs for the vesicle-bound fraction. This assumption is supported by the rate behavior; the amplitude of the fast-decaying component (85%) corresponds to the fraction of $ZnTPPS^{4-}$ that is vesicle-bound (80 ± 5%), and the relaxation time for the slowly decaying component corresponds to the intrinsic decay rate of $^3ZnTPPS^{4-}$. No changes were detected in the transient or ground-state absorption spectra or intermediate decay rates after exposure to more than 100 laser flashes, indicating that, if oxidative quenching is the mechanism, it was followed quantitatively by the reaction:

$$ZnTPPS^{3-} + SP^{\bullet -} \rightarrow ZnTPPS^{4-} + SP \qquad (4)$$

The extinction coefficient of the $ZnTPPS^{3-}$ π-cation radical at 460 nm is about one-third of the value for $^3ZnTPPS^{4-}$; nonetheless, there was no evidence for accumulation of $ZnTPPS^{3-}$ during $^3ZnTPPS^{4-}$ decay. Thus, either quenching is not oxidative or, consistent with the thermodynamic potentials, back-electron transfer (reaction 4) is more rapid than the oxidative quenching step (reaction 3).

Quenching of $^3ZnTPPS^{4-}$ by AQ, SP−AQ, and SP−AQ−C_{12}. Biexponential decay of $^3ZnTPPS^{4-}$ was also observed when AQ or its SP-linked analogues were incorporated into PC vesicles. In these systems, the relaxation time of the fast decaying component (τ_1) was ~10-fold smaller than that for SP at equivalent loadings (Figure 8). As before, the magnitude of τ_2 corresponded to the intrinsic relaxation time of $^3ZnTPPS^{4-}$ and, for all reactions, $A_1/(A_1 + A_2) = 0.7-0.9$. In contrast, the relaxation rate for the fast component was dependent upon the identity of the quinone, with $\tau_1 = 30$ μs (AQ), 20 μs (SP−AQ), and 150 μs (SP−AQ−C_{12}) under conditions equivalent to those given in Figure 8. The relatively slow quenching rate constant for SP−AQ−C_{12} is consistent with conclusions drawn from transient absorption spectra that this compound is bound relatively deeply within the hydrocarbon bilayer (Figure 3). Biphasic kinetics with nearly identical rate parameters were also observed when the SP−AQ doped PC vesicles were preilluminated with UV light to convert 30−35% of the dye to the mero form, i.e., $\tau_1 = 25$ μs and 180 μs, respectively, for MC−AQ and MC−AQ−C_{12}-containing vesicles, indicating that the quenching reaction was insensitive to the isomeric state of the dye. Thus, in these assemblies as well, the fast step corresponds to reactions of PC-bound $^3ZnTPPS^{4-}$, and the slow step, to decay of the unbound fraction of the zinc porphyrin.

The decay of $^3ZnTPPS^{4-}$ at 460 nm was accompanied by a transient increase in absorbance at wavelengths above 600 nm; because this absorption was relatively weak, it was not possible to determine from the transient spectrum the identity of the intermediate, which could be either $ZnTPPS^{3-}$ or $ZnTPPS^{5-}$.[39] However, two lines of evidence strongly suggest that this species is $ZnTPPS^{3-}$, formed by oxidative quenching by the anthraquinone moiety, e.g.,

$$^3ZnTPPS^{4-} + SP-AQ \rightarrow ZnTPPS^{3-} + SP-AQ^{\bullet -} \qquad (5)$$

First, the increase in decay rate was observed in all cases where the AQ group was present, implying the presence of an additional decay channel, i.e., reaction 5. Given the large rate enhancement, this must be the most important pathway under the experimental conditions. Consistent with the relatively large quenching rate, reaction 5 is predicted from the thermodynamic potentials given in Figure 6 to be slightly exothermic (ΔE = 40 mV). Second, disappearance of the transient was accelerated in the presence of EDTA by a reaction that was first-order in the electron donor concentration. The reported porphyrin potential $E°(ZnTPPS^{3-/4-}) = 0.87$ V[20]) is very similar to potentials for EDTA estimated from electrochemical data,[23,40] so that the reaction

$$ZnTPPS^{3-} + EDTA \rightarrow ZnTPPS^{4-} + EDTA^{+} \qquad (6)$$

should be nearly isoenergetic. Under the experimental conditions used (5 mM EDTA, 2 μM $ZnTPPS^{4-}$, 5 mg/mL PC, 20−100 mJ/pulse), reductive quenching of $^3ZnTPPS^{4-}$ was negligible. The bimolecular rate constant calculated for reaction 6 from the enhanced rates of transient decay at 650 nm was $k_6 \approx 10^5$ M^{-1} s^{-1}.

In the absence of exogenous electron donors, $ZnTPPS^{3-}$ underwent first-order decay to regenerate the original absorption spectrum; these relaxation times were moderately dependent upon the identity of the vesicle-bound AQ-containing compounds ($\tau \approx 100$ μs (SP−AQ−C_{12} or 30% MC−AQ−C_{12}), $\tau \approx 200$ μs (30% MC−AQ), $\tau \approx 300$ μs (SP−AQ), $\tau \approx 50$ μs (AQ)), presumably reflecting differences in back-electron-transfer rates between products of the oxidative quenching reaction, e.g.,

$$ZnTPPS^{3-} + SP-AQ^{\bullet -} \rightarrow ZnTPPS^{4-} + SP-AQ \qquad (7)$$

The reaction of SP−AQ with $^3ZnTPPS^{4-}$ in methanol exhibited qualitatively similar dynamical behavior to the reactions of vesicle-bound SP−AQ. Specifically, an EDTA-reactive transient intermediate was detected, whose spectrum was consistent with $^3ZnTPPS^{4-}$; from the second-order decay rate of the intermediate, measured at either 460 or 650 nm, a back-electron-transfer rate constant of $k_7 = 6 \times 10^9$ M^{-1} s^{-1} was calculated. Rate parameters for the various reactions studied are collected in Table 1.

Photosensitized Transmembrane Oxidation−Reduction. One-electron reduction of $Co(bpy)_3^{3+}$ by EDTA, i.e.,

$$EDTA + Co(bpy)_3^{3+} \rightarrow EDTA^{+} + Co(bpy)_3^{2+} \qquad (8)$$

Table 1. Apparent Redox Rate Constants for PC-Bound Reactants Measured by Transient Spectrophotometry

reaction	k[a]
$^3ZnTPPS^{4-} \rightarrow ZnTPPS^{4-}$	$5 \times 10^2\ s^{-1}$
$^3ZnTPPS^{4-} + SP \rightarrow ZnTPPS^{3-} + SP^{\bullet-}$	$\leq 2 \times 10^3\ s^{-1}$
$^3ZnTPPS^{4-} + AQ \rightarrow ZnTPPS^{3-} + AQ^{\bullet-}$	$3 \times 10^4\ s^{-1}$
$^3ZnTPPS^{4-} + SP{-}AQ \rightarrow ZnTPPS^{3-} + SP{-}AQ^{\bullet-}$	$5 \times 10^4\ s^{-1}$
$^3ZnTPPS^{4-} + SP(MC){-}AQ \rightarrow ZnTPPS^{3-} + SP(MC){-}AQ^{\bullet-}$ [b]	$4 \times 10^4\ s^{-1}$
$^3ZnTPPS^{4-} + SP{-}AQ{-}C_{12} \rightarrow ZnTPPS^{3-} + SP{-}AQ^{\bullet-}{-}C_{12}$	$7 \times 10^3\ s^{-1}$
$^3ZnTPPS^{4-} + SP(MC){-}AQ{-}C_{12} \rightarrow ZnTPPS^{3-} + SP(MC){-}AQ^{\bullet-}{-}C_{12}$ [b]	$6 \times 10^3\ s^{-1}$
$ZnTPPS^{3-} + EDTA \rightarrow ZnTPPS^{4-} + EDTA^{\bullet+}$	$1 \times 10^5\ M^{-1}\ s^{-1}$ [c]
$AQ^{\bullet-} + \{Co(bpy)_3^{3+}\}_i \rightarrow AQ + \{Co(bpy)_3^{2+}\}_i$ [d,e]	$1.5 \times 10^2\ s^{-1}$
$SP{-}AQH^{\bullet+}\ \{Co(bpy)_3^{3+}\}_i \rightarrow SP{-}AQ + \{Co(bpy)_3^{2+}\}_i + H^+_i$ [d,f]	$7 \times 10^2\ s^{-1}$
$SP(MC){-}AQ^{-\bullet} + \{Co(bpy)_3^{3+}\}_i \rightarrow SP(MC){-}AQ + \{Co(bpy)_3^{2+}\}_i$ [b,d,e]	$2 \times 10^2\ s^{-1}$
$SP{-}AQ^{\bullet-}{-}C_{12} + \{Co(bpy)_3^{3+}\}_i \rightarrow SP{-}AQ{-}C_{12} + \{Co(bpy)_3^{2+}\}_i$ [d,f]	$2 \times 10^2\ s^{-1}$
$SP(MC){-}AQ^{\bullet-}{-}C_{12} + \{Co(bpy)_3^{3+}\}_i \rightarrow SP(MC){-}AQ{-}C_{12} + \{Co(bpy)_3^{2+}\}_i$ [b,d,e]	$5 \times 10^1\ s^{-1}$

[a] At 23 °C, determined from relaxation times under the prevailing conditions as described in the text. [b] Vesicles contained 30−35% of the merocyanine form. [c] Apparent value, determined under the conditions given in Figure 8. [d] Rate-limited by semiquinone-mediated transmembrane redox. [e] As written, electrogenic. [f] As written, electroneutral.

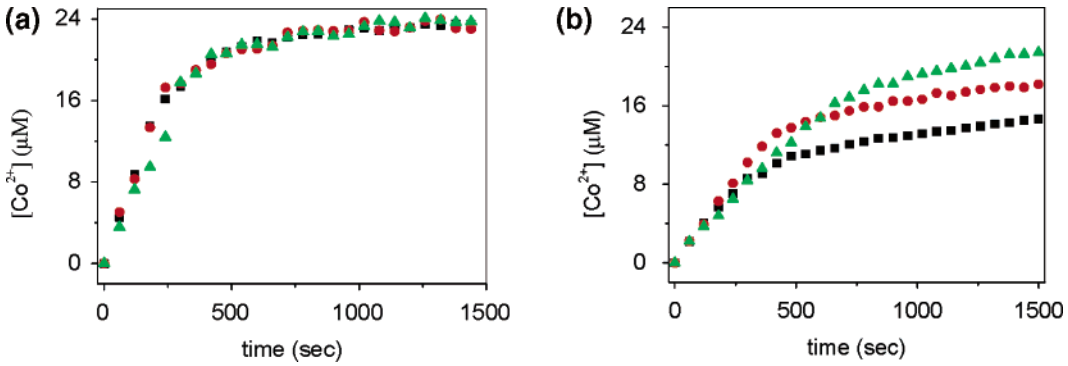

Figure 9. $Co(bpy)_3^{2+}$ accumulation monitored at 320 nm under continuous illumination of the $ZnTPPS^{4-}$ Soret band. Conditions: $[Co(bpy)_3^{3+}] = 25\ \mu M$, $[ZnTPPS^{4-}] = 2\ \mu M$, [EDTA] = 5 mM, [PC] ≈ 80 nM (5 mg/mL), and [quinone] = 2 μM in 40 mM Tris/Cl, pH 8.0. (a) SP−AQ (black squares) plus 20 μM CCCP (red circles) or 40 μM CCCP (green triangles); (b) SP−AQ−C_{12} (black squares) plus 20 μM CCCP (red circles) or 40 μM CCCP (green triangles).

is substantially enderogonic, based upon the reported potential of $E°(Co(bpy)_3^{3+/2+}) = 0.35$ V[41] and an estimated potential of ≈ 1V for one-electron oxidation of EDTA obtained from electrochemical data.[23,40]. Consistent with these potentials, EDTA and $Co(bpy)_3^{3+}$ are unreactive when mixed in aqueous solutions. However, net $ZnTPPS^{4-}$-photosensitized one-electron transfer was observed under certain conditions between EDTA contained in the bulk medium and $Co(bpy)_3^{3+}$ occluded within the inner aqueous compartments of PC vesicles. Specifically, this reaction required the presence of AQ or an AQ-containing compound within the bilayer; substitution of SP or SP/MC mixtures or omission of any of the reaction components completely blocked $Co(bpy)_3^{2+}$ formation. Representative results obtained under continuous illumination of the $ZnTPPS^{4-}$ Soret band are displayed in Figure 9, which illustrates the dependence of the overall reaction rate upon the identity of the quinone-containing molecule.

Laser-flash spectrophotometry made in the presence of EDTA revealed the appearance of weakly absorbing long-lived transient species at 590 nm, whose decay was markedly accelerated when the vesicles contained occluded $Co(bpy)_3^{3+}$ (Figure 10). This wavelength is nearly isosbestic for $ZnTPPS^{4-}$ and either $ZnTPPS^{3-}$ or $ZnTPPS^{5-}$ [39] but is a region where the semiquinone absorbs strongly.[42] These data were analyzed according

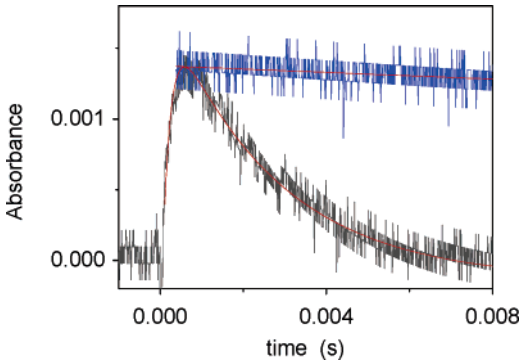

Figure 10. Formation and decay of transient absorption at 590 nm following photoexcitation of $ZnTPPS^{4-}$ in (SP−AQ)-containing PC vesicles without occluded $Co(bpy)_3^{3+}$ (blue line) or with $[Co(bpy)_3^{3+}] = 25$ mM (black). The red line is the best fit of experimental data using the equation and parameters given in the text [EDTA] = 6 mM; other conditions are the same as those given in Figure 7.

to the following equation: $A_{590}(t) = A_1(1 - \exp(-t/\tau_1) + A_2 \exp(-t/\tau_3)$, where the first and second terms are taken to be the formation and decay of $AQ^{\bullet-}$ species, respectively. The best-fit value for τ_1 (Figure 10) is 20 μs, corresponding to the relaxation time measured for $^3ZnTPPS^{4-}$ decay. Best-fit values obtained for τ_3 were 1.5 ms and ∼130 ms in the presence and absence of $Co(bpy)_3^{3+}$, respectively; analyses of analogous experiments with AQ and SP−AQ−C_{12} gave τ_3 values of 6.8 and 6.4 ms, respectively, in the presence of $Co(bpy)_3^{3+}$. Remarkably, 30−35% conversion to the mero forms caused τ_3

(39) Neta, P. *J. Phys. Chem.* **1981**, *85*, 3678−3684.
(40) Štulík, K.; Vydra, F. *J. Electroanal. Chem.* **1968**, *16*, 385−395.
(41) Farina, R.; Wilkins, R. G. *Inorg. Chem.* **1968**, *7*, 514−518.
(42) Buschel, M.; Stadler, C.; Lambert, C.; Beck, M.; Daub, J. *J. Electroanal. Chem.* **2000**, *484*, 24−32.

to increase severalfold, i.e., to 5.0 ms for MC−AQ and 20 ms for MC−AQ−C_{12} in the presence of $Co(bpy)_3^{3+}$ (Table 1). Based upon the AQ/$AQ^{\bullet-}$ reduction potential measured in DMSO, electron transfer to $Co(bpy)_3^{3+}$ is highly exergonic, with $\Delta E = 1.5$ V.[43] Given that τ_3 was 20−90-fold smaller when $Co(bpy)_3^{3+}$ was occluded within the vesicles, τ_3 must be a good approximation under these conditions to the relaxation time for transmembrane reduction by an externally generated AQ semiquinone radical, i.e.,

$$SP-AQ^{\bullet-}\ (\text{or } SP-AQH^{\bullet})_o + (Co(bpy)_3^{3+})_i \rightarrow SP-AQ + (H^+)_i + (Co(bpy)_3^{2+})_i \quad (9)$$

Because exergonic one-electron reduction of $Co(bpy)_3^{3+}$ in homogeneous solution is very rapid,[44] it also follows that the relatively slow redox reaction measured as τ_3 in these assemblies is rate-limited by the transmembrane charge separation step.

The redox mechanism(s) could involve any combination of electroneutral processes such as transmembrane diffusion of AQH-containing carriers following uptake of a proton from the external aqueous−organic interface and electrogenic processes such as transmembrane diffusion of $AQ^{\bullet-}$-containing carriers or AQ/$AQ^{\bullet-}$ electron exchange, leading to net translocation of the electron across the bilayer. In closed bilayer membranes, electrogenic processes can often be distinguished from electroneutral processes by the self-impeding nature of the former reactions.[44,45] Specifically, electron transport that is uncompensated electrostatically by movement of other charges across the bilayer will generate a transmembrane potential that opposes further movement of charge as the reaction proceeds; this developing potential leads to marked diminution in rate in the latter stages of the reaction. Providing a pathway for movement of charge-compensating ions, e.g., by adding an ionophoric compound, will collapse the potential and accelerate transmembrane charge transport. However, if the reaction is electroneutral, no transmembrane potential will develop and addition of an ionophore will have negligible effect on the transport process. Examples of both types of behavior are illustrated in Figure 9. In panel a, internal $Co(bpy)_3^{3+}$ was relatively rapidly and completely reduced under continuous illumination of the $ZnTPPS^{4-}$ photosensitizer when SP−AQ was the membrane charge carrier, whereas the corresponding reaction using SP−AQ−C_{12} (panel b) was only ∼50% complete over the same illumination period and was characterized by a rapidly attenuating rate of reaction. Addition of the proton transporter carbonyl cyanide *m*-chlorophenylhydrazone (CCCP) accelerated both rates of formation and yields of $Co(bpy)_3^{2+}$ in the latter case (Figure 9b) but had no effect upon transmembrane redox when SP−AQ was the carrier (Figure 9a). Very similar results were obtained when CCCP was replaced by the K^+-selective ion transporter valinomycin in K^+-buffered media; however, addition of valinomycin to Na^+-buffered media did not affect the time course of $Co(bpy)_3^{3+}$ reduction, consistent with a mechanism whereby valinomycin collapses the developing electrochemical potential by selective transmembrane transport of K^+.[46] Reactions using vesicles that contained AQ or MC−AQ as redox mediators also exhibited dynamical properties under continuous illumination associated with electrogenic charge transport, i.e., rate acceleration in the latter stages of the reaction in the presence of CCCP or K^+-valinomycin. In contrast, although the rate profile and extent of $Co(bpy)_3^{3+}$ reduction in MC−AQ−C_{12}-containing vesicles were consistent with electrogenic electron transport, the reaction rates were not appreciably accelerated by adding CCCP. It is possible that, at the very low dopant loadings used in these studies, a significant side reaction of this relatively immobile semiquinone depleted the carrier concentration and thereby lowered transport fluxes. Disproportionation of the semiquinone radical, i.e., 2 MC−AQ−$C_{12}^{\bullet-}$ + $2H^+$ → MC−AQ−C_{12} + MC−AQH_2−C_{12}, may contribute to loss of the functioning carrier; the hydroquinone, anthracene-9,10-diol (AQH_2), when solubilized in PC vesicles, reacted only very slowly with $Co(bpy)_3^{3+}$ present in the external medium ($t_{1/2} \approx 1-2 \times 10^4$ s, $[AQH_2] = 10-20$ μM, $[Co(bpy)_3^{3+}] = 20-30$ μM, 23 °C), consistent with a high energetic barrier for one-electron oxidation to the semiquinone.

The relaxation times for decay of the 590 nm transients (Figure 10) are very similar to τ-values previously measured for the corresponding reactions of uncharged *N*-alkyl-4-cyanopyridinium radicals,[19] whereas diffusion of lipophilic ions such as *N*,*N*-dialkyl-4,4,-bipyridinium monocation radicals is generally several orders of magnitude slower.[44] Thus, the transmembrane redox rates are compatible with SP−AQ functioning as a neutral cotransporter of electrons and protons, i.e., as SP−AQH, but not with the semiquinone ions as mobile electron transporters, i.e., as $AQ^{\bullet-}$ and SP−$AQ^{\bullet-}$−C_{12}. More likely, electronic charge in these cases is transported by AQ−$AQ^{\bullet-}$ exchange, or site-to-site electron hopping, across the bilayer. The physical basis for the apparent difference in mechanisms between SP−AQ and AQ or SP−AQ−C_{12} may reside in limited access of the latter quinones to the membrane aqueous−organic interface which, for AQ, is a consequence of its extreme lipophilicity and, for SP−AQ−C_{12}, reflects the immobilizing effect of its dodecanyl "anchor". We have noted very similar effects of appending long alkyl chains to mobile viologens that can function as electron transporters across bilayer membranes, i.e., conversion from an electroneutral to an electrogenic mechanism with addition of lipophilic ions being required to achieve complete reaction.[47] The influence of membrane micropolarity might also account for the ∼3-fold decrease in the transmembrane redox rate constant that accompanies partial conversion of SP to MC in the SP−AQ compounds (Table 1). Specifically, the open-ring merocyanine form is more polar than the closed-ring spiropyran form (Scheme 1), so that the hydrocarbon interior of the membrane presents a greater

(43) Although the membrane interior presents a complex microheterogeneous environment, the measured one-electron quinone potential in DMSO should be a good approximation to the actual potential in PC membranes. Specifically, polarographically determined values for the AQ/$AQ^{\bullet-}$ potential in various aprotic solvents were relatively independent of solvent dielectric constant (ϵ), varying by less than 200 mV over a range of $\epsilon = 13-47$, with a reported value of $E_{1/2} = -1.28$ V (vs $Fc^{+/0}$) in DMSO [Jaworski, J. S.; Lesniewska, E.; Kaliowski, M. K. *J. Electroanal. Chem.* **1979**, *105*, 329−334]. Moreover, ab initio calculations made in the course of these studies gave values for the potential that were virtually independent of dielectric strength over the range $\epsilon = 78-21$ ($E^\circ = -1.36$ to -1.42 V (vs $Fc^{+/0}$)), corresponding to the aqueous−organic interfacial region of the membrane. At lower ϵ, the calculated reduction potential became progressively more negative, reaching $E^\circ = -1.78$ V when $\epsilon = 4.9$, corresponding to the hydrophobic membrane interior. Results of the computations are appended as Supporting Information.

(44) Lymar, S. V.; Hurst, J. K. *J. Phys. Chem.* **1994**, *98*, 989−996.

(45) Hurst, J. K. In *Kinetics and Catalysis in Microheterogeneous Media*; Gratzel, M., Kalyanasundaram, K., Eds.; Surfactant Science Series, Vol. 38; Marcell Dekker: New York, 1991; pp 183−226.

(46) Nicholls, D. G.; Ferguson, S. J. *Bioenergetics 3*; Academic Press: New York, 2002.

(47) Patterson, B. C.; Hurst, J. K. *J. Phys. Chem.* **1993**, *97*, 454−465.

Table 2. Kinetic Parameters for Quinone-Mediated Transmembrane Redox[a]

compound	φ[b]	$\tau_5^{-1}/(\tau_5^{-1}+\tau^{-1})$	τ_7 (ms)	τ_8 (ms)	X[c]	Φ_{calcd}	Φ_{exptl}
AQ	0.73	0.99	0.05	0.8	0.26	0.06	0.0345
SP−AQ	0.48	0.99	0.3	1.5	0.26	0.12	0.071
MC−AQ[d]	0.24	0.99	0.2	5.0	0.12	0.0285	0.012
SP−AQ−C_{12}	0.74	0.93	0.1	6.4	0.065	0.045	0.034
MC−AQ−C_{12}[e]	0.58	0.92	0.1	20	0.052	0.028	0.013

[a] Conditions: $[ZnTPPS^{4-}] = 2\ \mu M$, [EDTA] = 5 mM, [quinone] = 2 μM, $[Co(bpy)_3^{3+}]_i = 25\ \mu M$, [PC] ≈ 80 nM (5 mg/mL) in 40 mM Tris/Cl, pH 8.0, 23 °C. [b] Corrected for fluorescence from unbound fraction (20%) of $^1ZnTPPS^{4-}$ as indicated in the text. [c] $X = (k_6[EDTA] + \tau_9^{-1})/(k_6[EDTA] + \tau_7^{-1} + \tau_9^{-1})$. [d] 0.7 μM MC−AQ + 1.3 μM SP−AQ. [e] 0.6 μM MC−AQ−C_{12} + 1.4 μM SP−AQ−C_{12}.

energetic barrier to its transmembrane diffusion. Similarly, electron transfer from MC−$AQ^{\bullet-}$−C_{12} to SP−AQ−C_{12} could be energetically unfavorable within the membrane because it involves transfer of charge into a less polar microenvironment. This latter effect would not be evident from comparisons of potentials in homogeneous solution.

Quantum Yields for Transmembrane Redox. Overall quantum yields for transmembrane oxidation−reduction were determined from the initial rates of $Co(bpy)_3^{3+}$ disappearance, as described in the Experimental Section. To examine the effect of partial conversion of the dyes to their mero forms, photoexcitation of the $ZnTPPS^{4-}$ sensitizer at 420 nm was preceded by 10−15 min of broadband UV illumination (260−390 nm). Under these conditions, 30−35% of the bound dye was converted to the mero form, as determined from the steady-state optical absorption spectra. Quantum yields measured under an equivalent set of conditions are listed in Table 2; the values decrease upon partial conversion to the mero form and upon addition of an alkyl chain to the molecule. The quantum yields were analyzed quantitatively by considering the individual reactions investigated in this study, including fluorescence quenching of $^1ZnTPPS^{4-}$ (Figure 5) and reactions 5−7 and 9. Reactions 3 and 4 were not explicitly considered because it was evident from the transient decay profiles (cf., Figures 7 and 8) that quenching of $^3ZnTPPS^{4-}$ by the AQ moiety was far more efficient than either SP or MC. With the further assumptions that only the vesicle-bound fraction of the photoexcited $ZnTPPS^{4-}$ reacted with the dye and that semiquinone capable of functioning as a redox mediator was formed only by oxidative quenching of $^3ZnTPPS,^{4-}$ the quantum yield for $Co(bpy)_3^{3+}$ reduction (Φ) is given by:

$$\Phi = \varphi \times k_5[SP-AQ]/(k_5[SP-AQ] + \tau^{-1}) \times (k_6[EDTA] + \tau_9^{-1})/(k_6[EDTA] + \tau_7^{-1} + \tau_9^{-1}) \quad (10)$$

where φ is the quantum yield for $^3ZnTPPS^{4-}$ formation and τ = 2.1 ms is the intrinsic lifetime of $^3ZnTPPS^{4-}$. The second right-hand term in eq 10 is the fraction of $^3ZnTPPS^{4-}$ that undergoes oxidative quenching and the third term is the fraction of the semiquinone formed that escapes recombination with $ZnTPPS^{3-}$ to reduce $Co(bpy)_3^{3+}$. The value of φ was calculated from the equation: $\varphi = \Phi_s \times \Phi_t$, where Φ_s is the fraction of bound $^1ZnTPPS^{4-}$ that does not undergo static quenching, and Φ_t is the quantum yield for singlet−triplet intersystem crossing of $^1ZnTPPS^{4-}$. For these calculations, Φ_t was assigned a value of 0.84,[20] and Φ_s was estimated from fluorescence quenching data measured under the prevailing conditions after correcting for the fluorescence arising from unbound $^1ZnTPPS^{4-}$ (Figure 5). For this correction, the relative fluorescence quantum yield of $^1ZnTPPS^{4-}$ in buffer was determined to be ∼46% of that of the PC-bound zinc porphyrin. Calculated values of Φ are listed in Table 2, along with the parameters used in the calculations. Given the large number of parameters involved, whose experimental uncertainties are ±10−40%, the correspondence between directly measured and calculated overall quantum yields is good; in particular, experimentally determined trends involving individual redox carriers are accurately reproduced.

Mechanistic Conclusions. The quantum yields for transmembrane charge transfer in these assemblies are relatively low but consistent with earlier studies where it was found that photosensitized transmembrane redox was efficient only when the systems were organized so that oxidative quenching occurred in the bulk aqueous phase or across the organic-aqueous interface of the membrane, i.e., from free $^3ZnTPPS^{4-}$ to vesicle-bound quencher.[19,28,48] In the present case, examination of the individual reaction steps revealed that the low quantum yields was a consequence primarily of two factors, unproductive quenching of $^1ZnTPPS^{4-}$ by the SP and MC groups on the dye and relatively efficient back-electron transfer between the semiquinone and $ZnTPPS^{3-}$ formed by oxidative quenching of $^3ZnTPPS^{4-}$ by AQ, SP−AQ, or SP−AQ−C_{12} (Table 2). In contrast, oxidative quenching of $^3ZnTPPS^{4-}$ by the AQ moiety occurred with near-unitary efficiency under the experimental conditions. The 6-fold decrease in overall quantum yield for transmembrane redox observed when SP−AQ was partially converted to the MC form is also the product of two factors: 2-fold reduction in φ, indicating more efficient quenching of $^1ZnTPPS^{4-}$ by MC−AQ, and a 3-fold slower transmembrane redox step (Table 1). The lower overall quantum yield for SP−AQ−C_{12} compared to SP−AQ is attributable to its much lower transmembrane charge-transfer rate, since, in this case, fluorescence quenching was less extensive. The (2−3)-fold reduction in overall quantum yield observed upon partial conversion to MC−AQ−C_{12} can also be attributed to a combination of increased $^1ZnTPPS^{4-}$ quenching and lower transmembrane charge-transfer rate.

Acknowledgment. The authors gratefully acknowledge helpful discussions with Drs. David M. Kramer (WSU), Scot Wherland (WSU), and C. Michael Elliott (Colorado State) concerning determination of nonaqueous potentials. Financial support was provided by the Division of Chemical Sciences, Office of Basic Energy Sciences, U.S. Department of Energy, under Grant DE-FG03-99ER14943.

Supporting Information Available: Tabulations of ^{13}C NMR peaks for the synthesized compounds and the calculated one-electron reduction potentials for an SP−AQ analogue. This material is available free of charge via the Internet at http://pubs.acs.org.

JA0545620

(48) Khairutdinov, R. F.; Hurst, J. K. *J. Am. Chem. Soc.* **2001**, *123*, 7352−7359.